High-Pressure Laser Photolysis Study of Hemoproteins. Effects of Pressure on Carbon Monoxide Binding Dynamics for R- and T-State Hemoglobins†

Masashi Unno, Koichiro Ishimori, and Isao Morishima*
Division of Molecular Engineering, Graduate School of Engineering, Kyoto University, Kyoto 606, Japan
Received December 7, 1989; Revised Manuscript Received July 23, 1990

ABSTRACT: The bimolecular association reaction of carbon monoxide to human adult hemoglobin at pH 7, 20 °C, was examined as a function of pressure up to 1500 bar by means of high-pressure laser photolysis. The apparent quantum yield for a millisecond recombination reaction decreased with pressure, which was attributed to an increase in the fraction of nanosecond geminate recombination reaction. On the basis of the pressure dependence of the recombination rate, the activation volumes at normal pressure for the binding of carbon monoxide to the R- and T-state hemoglobins were determined as -9.0 ± 0.7 and -31.7 ± 2.4 cm^3 mol^{-1}, respectively. Since the activation volumes for the overall CO association reaction were negative, it seems that the iron–ligand bond formation process mainly contributes to the rate-limiting step for both quaternary structures. The characteristic pressure dependence of the activation volume was observed for the R-state Hb but not for the T-state Hb. At 1000 bar, the activation volume for the R-state Hb was reduced to nearly zero, probably resulting from the contribution of the ligand migration process to the rate-limiting step. The effect of pressure on the activation enthalpy and entropy was also extracted from the data.

X-ray crystallographic studies of human adult hemoglobin (Hb A) have revealed two distinct quaternary structures, the fully deoxygenated Hb with T-state structure and the fully liganded (oxy, carboxy, nitroxy, etc.) Hb with R-state structure (Perutz, 1980; Baldwin & Chothea, 1979). In going from the deoxy-Hb T-state to the liganded Hb R-state, large configurational or structural changes are induced at the subunit interface and heme active site as well. Many of the cooperative ligand binding features in Hb have been accounted for by assuming that there is an equilibrium between the low ligand affinity T and the high ligand affinity R structures.

One of the key issues to be addressed by the structural model of Hb allostery is the elucidation of the different features of the ligand binding mechanism between the R- and T-state Hbs. Transient absorption studies have been shown particularly useful for delineating the mechanism of the ligand binding reaction of Hb. On the millisecond time scale, two relaxations have been observed, which are bimolecular rebinding of ligand from the solvent to the R and T quaternary structures with time constants of about 200 μs and 10 ms, respectively (Murray et al., 1988a,b). The difference in affinity of the R- and T-state Hb to carbon monoxide may be manifested mainly in this rebinding rate (Sawicki & Gibson, 1976; Szabo, 1978). In the nanosecond region, the geminate CO rebinding rate of about 50 ns was observed (Duddel et al., 1979, 1980; Alpert et al., 1979; Friedman & Lyons, 1980; Catteral et al., 1982; Hofrichter et al., 1983; Campbell et al., 1984, 1985). This nanosecond rebinding is the process by which the photodissociated ligand rebinds to the heme iron without having diffused into the surrounding solvent. From these nanosecond studies, the three-species model has been proposed (Campbell et al., 1984). According to this model, there are two elementary steps in the bimolecular association reaction for each quaternary structure. The first step is entry of the ligand into the heme pocket, followed by ligand binding to the heme.

Despite the fact that the ligand binding kinetics of Hb has been extensively studied, several important questions about the ligand binding mechanism, especially concerning the ligand binding dynamics, remain to be answered. One of the most uncompromising problems that we encounter in studying the ligand binding mechanism is the difficulty of directly characterizing the intermediate states in the ligand binding dynamics in terms of protein structures. In this paper, we describe a high-pressure laser photolysis study of carbonmonoxy-Hb A to elucidate the dynamical aspect of the ligand binding to Hb.

The effects of pressure on the structures of some hemoproteins have been studied by use of UV/vis absorption (Weber & Drickamer, 1983; Ogunmola et al., 1977; Alden et al., 1989), magnetic susceptibility (Messana et al., 1978), NMR spectroscopy (Morishima et al., 1979, 1980; Morishima & Hara, 1982, 1983), and resonance Raman spectroscopy (Alden et al., 1989). The influence of pressure on the ligand binding kinetics for some hemoproteins has also been studied (Hasinoff, 1974; Caldin & Hasinoff, 1975; Adachi & Morishima, 1989; Projahn et al., 1990; Frauenfelder et al., 1990). These pressure-dependent kinetic studies provide information on the volume profile of the ligand binding process. The activation volume, the difference in partial molar volume between the activated complex and the reactants, is very easily visualized and is sensitive to the dynamics associated with the reaction process. Here we present a study of the effects of pressure (up to 800–1500 bar) on the bimolecular CO rebinding to Hb A to characterize the intermediate states in the ligand binding reaction for the R and T quaternary Hbs.

Materials and Methods

Preparation of Hemoglobin. Hemolysate was prepared by a standard method from whole blood samples obtained from a local blood bank. Hb A was prepared in the carbon monoxide form as described by Ishimori and Morishima (1988). Hb A was stored in the carbonmonoxy form in liquid nitrogen prior to use. All of the experiments were performed in 50 mM Tris buffer at pH 7, which contains 0.1 M Cl^-. This buffer

† This work is supported by a grant from the Ministry of Education, Science and Culture, Japan (62840013).
* To whom correspondence should be addressed.

0006-2960/90/0429-10199$02.50/0

has been shown to exhibit no pressure dependence of pH in the pressure region examined here (Neuman et al., 1973). The protein concentration was varied from 25 to 40 μM (heme), and it was determined as carboxyhemoglobin, with a millimolar extinction coefficient of 13.4 mM^{-1} at 540 nm on a heme basis. The CO concentration was based on a Henry's law coefficient of 1.04 mM atm^{-1}.

Millisecond Laser Photolysis Measurements under High Pressures. Excitation light was obtained from a lamp pumped dye laser (UNISOKU LA-501) with Rhodamine 6G (Kodak) dye solutions. We used a 50 μM solution of Rhodamine 6G in methanol, and the laser produced 250-mJ pulses. The pulse half-width was 300 ns. At atmospheric pressure, 10-mm path-length cells were used. The absorption spectra were monitored at a right angle to the excitation source on a monochrometer, UNISOKU USP-501, and detected by a photomultiplier. A transient recorder, Graphtec TMR-80, was used to digitize the signal (50 ns/point, 4096 points), and data were transferred to a NEC PC-9801VX computer for further analysis. The monitoring beam was generated by a pulsed xenon arc lamp and focused within the area of the laser beam at the surface of the sample. The monitoring wavelength was 436 nm, which is the isosbestic point for the R- and T-state Hbs (Sawicki & Gibson, 1976).

The high-pressure photolysis experiments were performed with a high-pressure cell, and its inner capsule was made of quartz. The inner sample capsule consists of the upper cylindrical part and the lower square-shaped part. The lower optical square-shaped part has a path length of 5.0 mm. The details of the high-pressure cell and its inner sample capsule are described elsewhere (Hara & Morishima, 1988). The pressure was transmitted from an intensifier (Hikari High-Pressure Co., Ltd. KP-5-B) and was measured with a Bourdon tube gauge.

Nanosecond Laser Photolysis Measurements under High Pressure. The second harmonic (347.2 nm) of a Q-switched ruby laser with a half-peak duration of 20 ns was used. The Xe lamp and the probe light were focused onto the entrance slit of a monochrometer and detected by a photomultiplier (HTV R666). An Iwatu storage oscilloscope was used to digitize the resulting signal. The high-pressure apparatus was the same as that for the millisecond laser photolysis measurements. The nanosecond photolysis experiments were performed at 1–1500 bar in 50 mM Tris–0.1 M Cl^-, pH 7, at room temperature (~20 °C) with a monitoring wavelength of 436 nm.

Evaluation of the Bimolecular Association Rate Constants. In the R-state Hb, Guggenheim plots were used for the rate constants, and they were fitted to

$$\ln (\Delta A_{t+dt} - \Delta A_{dt}) = -k_{app}t \quad (1)$$

in the time range of 0 to ~100 μs, where ΔA_t and ΔA_{t+dt} are the absorbance changes at any time t and $t + dt$, respectively. k_{app} is the observed pseudo-first-order rate constant; 40 μs was used for the value of dt.

The semilog plots were used for the T-state Hb, and they were fitted to eq 2 in the time range of 2–7 ms, where $\Delta A_{t=0}$

$$\ln (\Delta A_t - \Delta A_{t=0}) = -k_{app}t \quad (2)$$

is the initial absorbance change and ΔA_t is the absorbance change as a function of time.

Calculation of the Activation Volumes, Enthalpies, and Entropies. The activation volume is given by eq 3. R is the

$$\Delta V^{\ddagger} = -RT\,(\partial \ln k/\partial p) \quad (3)$$

gas constant (=8.314 J K^{-1} mol^{-1}) and 293.15 K was used for the value of T. The slope ($\partial \ln k/\partial p$) for the R-state Hb at atmospheric pressure was calculated from the optimized third-order polynomial function. Second-order functions were used for the function of the T-state Hb. Curve fits were performed from 1 to 1000 bar for both Hbs.

We assume that the CO ligation rate constant obeys the Arrhenius equation:

$$k = A \exp(-E_a/RT) \quad (4)$$

A is a frequency factor, E_a is an activation energy, and R is the gas constant. A and E_a are assumed to be temperature independent. Transition-state theory (Glasstone et al., 1941) gives the rate constant as given by eq 5, where $\Delta G^{\ddagger}$ is the

$$k = \nu \exp(-\Delta G^{\ddagger}/RT) \quad (5)$$

activation free energy between the initial state and the transition state and ν is an approximately constant factor. Expressing the activation free energy in terms of activation enthalpy and activation entropy leads to eq 6, where ν, $\Delta S^{\ddagger}$, and

$$k = \nu \exp(-\Delta S^{\ddagger}/R) \exp(\Delta H^{\ddagger}/RT) \quad (6)$$

$\Delta H^{\ddagger}$ are temperature independent and a value of

$$\nu = 10^{11}\ M^{-1}\ s^{-1} \quad (7)$$

was used for the second-order reaction (Austin et al., 1975). Comparison of eqs 4 and 6 gives

$$\Delta H^{\ddagger} = E_a,\ \Delta S^{\ddagger} = R \ln (A/\nu) \quad (8)$$

Rate constants were obtained at various temperature from ~5 to ~25 °C, and the activation enthalpy was estimated from the slope of the plots of rate constant versus $1/T$. The activation entropies were evaluated by use of eq 5–8 and the activation free energy, which was calculated from the optimized second- or third-order polynomial function.

Results

Pressure Effects on the Apparent Quantum Yield and the Fraction of R- and T-State Hemoglobins. Time courses of the absorption spectral changes for CO rebinding to Hb in the millisecond region at various pressures are shown in Figure 1. It is well documented that at normal pressure the initial portions of the time courses (0 to ~1 ms) correspond to CO recombination to the R-state Hb and the slower relaxations (~1 to ~3 ms) result from recombinations to the T-state Hb (Gibson, 1959a; Antonini & Brunori, 1971; Antonini et al., 1972; Schmelzer et al., 1972). The most characteristic feature of Figure 1 is the decrease in the degree of photodissociation (which is called the apparent quantum yield for the millisecond region) of HbCO at elevated pressures. Under this experimental condition, the apparent quantum yield at atmospheric pressure was about 0.8 (~80% photolysis). At 1000 bar, the absorbance changes were reduced to about half of that at 1 bar.

The decrease in the photodissociation for the millisecond region could result either from the decrease of the intrinsic photochemical yield or from the increase of the geminate rebinding. In an effort to determine whether or not the low apparent quantum yield is due to the nanosecond geminate recombination, we performed the nanosecond laser photolysis experiments under various pressures. Some typical recombination reactions under different pressure are shown in Figure 2. It is readily noticed that the portion of photodissociated CO quickly rebinding to the iron in the nanosecond region is larger at 1000 bar than at 1 bar. Unfortunately, we could not successfully obtain the rate constants fitting the observed

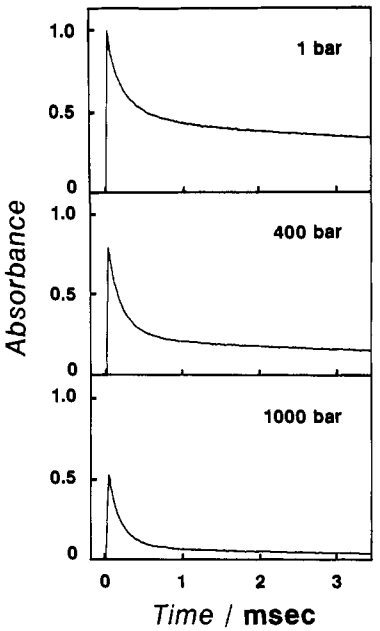

FIGURE 1: Millisecond time courses for recombination of 400 μM CO with human adult Hb at various pressure (1, 400, and 1000 bar). The reactions were carried out at 20 °C and pH 7 in 50 mM Tris–0.1 M Cl^- buffer and were monitored at 436 nm. Protein concentration was 37 μM (heme), and 5-mm path-length cells were used. Photolysis of HbCO was accomplished with a 300-ns laser flash (590 nm), and ~80% photolysis was obtained at atmospheric pressure.

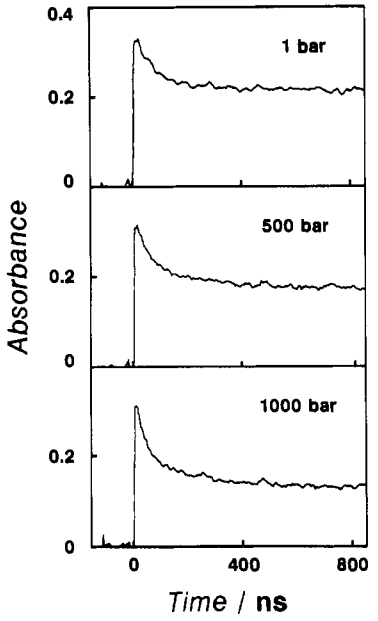

FIGURE 2: Nanosecond time courses for CO recombination with Hb at various pressure (1, 500, and 1000 bar). The reactions were carried out at room temperature (~20 °C) and pH 7 in 50 mM Tris–0.1 M Cl^- buffer and monitored at 436 nm. Protein concentration was 26.0 μM (heme), and 5-mm path-length cells were used. CO concentration was ~400 μM. Photolysis of the HbCO was accomplished with a 20-ns excitation pulse (347.2 nm). The geminate yields were as follows: 1 bar, 0.3; 500 bar, 0.4; 1000 bar, 0.5.

spectral time courses, which appear to be multiphasic. Therefore, we only determined the fraction of the geminate recombination, a geminate yield, preliminarily as a function of pressure. At atmospheric pressure, the geminate yield was about 0.3. The geminate yield was increased to about 0.4 and 0.5 at 500 and 1000 bar, respectively, while the millisecond CO rebinding fraction was decreased with rising pressure.

The difference in absorbance between carbonmonoxy- and deoxy-Hb at 436 nm was almost insensitive to pressure (figure not shown). Therefore, the low apparent quantum yield at high pressure is not caused by the pressure-induced absorbance changes for carbonmonoxy- and deoxy-Hb. Although quantitative comparison between the pressure-induced increase of the geminate rebinding and the decrease of the millisecond rebinding has not yet been made, it can be safely said that pressure does not affect so much the intrinsic photodissociation as does the laser power. In other words, pressure affects only the ratio of the nanosecond rebinding to the millisecond rebinding (geminate yield) and does not affect the intrinsic quantum yield.

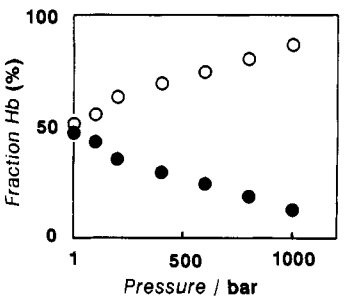

FIGURE 3: Pressure dependence of the fraction (as a percentage of photodissociated Hb) of the R- (○) and T-state Hb (●). The fraction of the T-state Hb was calculated from the extrapolated zero time absorbance changes by use of the logarithmic plots of Figure 1, and the R-state component fraction was evaluated from the difference between the photodissociated component fraction and the T-state one. The experimental conditions were described in Figure 1.

Figure 1 also shows that the spectral amplitude of the T-state species preferentially decreased with increased pressure. At 1000 bar, the recombination reaction appears to consist almost entirely of the fast phase. Figure 3 depicts the pressure effects on the fractions of the R- and T-state Hbs as a percentage of photodissociated Hbs. It shows that the fraction of the R-state Hb is increased from ~50 to ~90% and that of the T-state Hb is changed from ~50 to ~10% upon pressurization from 1 to 1000 bar. Therefore, the pressure-induced decrease in the apparent quantum yield for the millisecond rebinding can be mainly attributed to the decrease of the slow component of Hb (the T-state Hb).

Pressure Effects on the Bimolecular Association Rate Constants and the Kinetic Parameters. Time courses for CO association to the R- and T-state Hb are exemplified in Figures 4A and 5A, respectively. In Figure 4A, CO rebinds to the R-state Hb under normal and high pressure (1000 bar) in a buffer equilibrated with ~1 atm of CO. Partial photolysis experiments were performed to measure the bimolecular association rate constants for the R-state Hb, and the laser flash was attenuated to 15–50% photolytic breakdown. Under these conditions, CO rebinding to the R-state Hb is the main reaction (Gibson, 1959a). The time courses under all pressures are analyzed by the usual method of the Guggenheim plot, as shown in Figure 4B. The plot is linear at the initial stage in each reaction, implying that the reaction at the initial stage can be interpreted as the pseudo-first-order reaction. The bimolecular rate constant under normal pressure was evaluated as 9.1 ± 0.7 μM^{-1} s^{-1}. This value is in good agreement with those reported in the literature (Sawicki & Gibson, 1976).

Time courses at 1 and 600 bar in a buffer equilibrated with ~0.15 atm of CO are shown in Figure 5A and mainly represent the association kinetic behavior of the slow component, the T-state Hb. Since the laser flash was not reduced in this experiment, we got ~80% photolytic light. Under this experimental condition, the T-state Hb was chiefly obtained. The bimolecular association rate constants for CO rebinding to the T-state Hb were evaluated by the semilog plot method (Figure

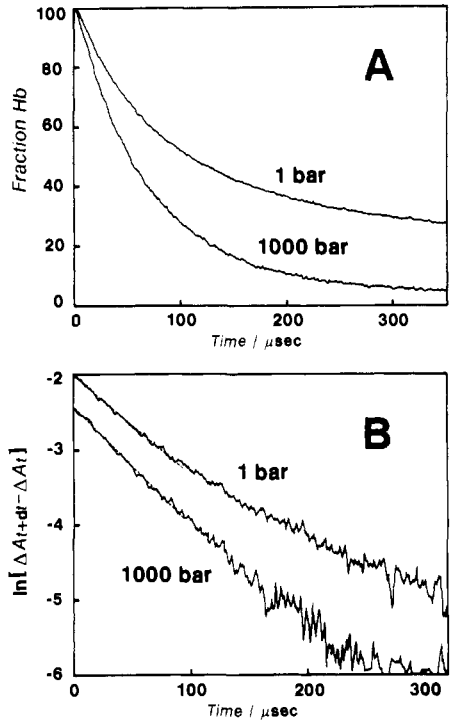

FIGURE 4: (A) Normalized time courses for the recombination of ~1 atm of CO with Hb following partial photolysis by a 300-ns laser flash under two different pressures. Partial photolysis was performed by use of an attenuated laser flash (~50–15% breakdown), and R-state Hb was mainly produced. The reactions were carried out at 20 °C, pH 7, in 50 mM Tris–0.1 M Cl^- buffers and were monitored at 436 nm. Protein concentration was 34–40 μM (heme), and 5-mm pathlength cells were used. (B) Guggenheim plot for the reactions as shown in (A). These plots were fitted in the time range of ~0–100 μs to eq 1. The dashed lines show the best fit to eq 1.

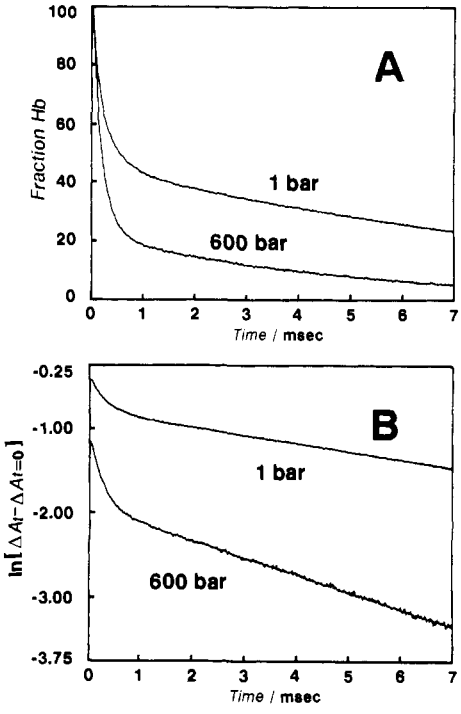

FIGURE 5: (A) Normalized time courses for the recombination of 0.15 atm of CO with Hb following photolysis by a 300-ns laser flash under two different pressures. Experimental conditions were described in Figure 4, and under these experimental conditions, T-state Hb was chiefly obtained. (B) Semilog plot for the reactions as shown in (A). These plots were fitted in the time range of 2–7 ms to eq 2. The dashed lines show the best fit to eq 2.

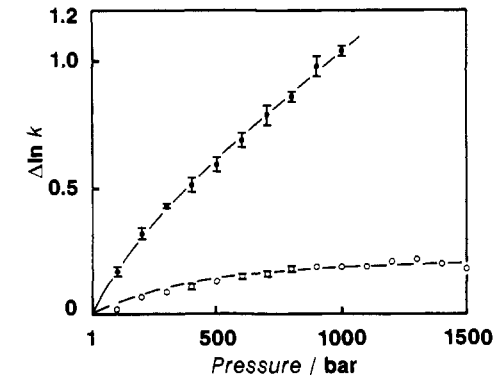

FIGURE 6: Logarithmic plots of the rate constants for the bimolecular CO association reaction versus pressure for the R- (○) and T-state Hb (●). Experiments were performed with millisecond laser photolysis apparatus in 50 mM Tris–0.1 M Cl^-, pH 7, at 20 °C. The points were determined as described in Figures 4 and 5 (see text), and the error bars are the standard deviation from the mean. Because the measurements for the R-state Hb under 1100–1500 bar were carried out only once, the error bars are not shown. The amplitude of the T-state Hb was markedly reduced by high pressure, so that the rate constants could not obtained above 1000 bar.

5B). The bimolecular rate constant for the T-state Hb at normal pressure was determined as 0.42 ± 0.02 μM^{-1} s^{-1}, which corresponds to the previous data (Sawicki & Gibson, 1976).

In order to delineate the pressure effects on the ligand binding reaction rate, k_{app}, Δ ln k [= ln k_p (at high pressure)/k_1(1 atm)] is plotted against pressure in Figure 6. The activation volume was determined from the slope, and the resulting activation volumes for both R- and T-state Hbs at atmospheric pressure are evaluated. There are two significant features as inspected. First, the CO rebinding process for the T-state Hb experiences a larger activation volume (−31.7 ± 2.4 cm^3 mol^{-1}) than that for the R-state Hb (−9.0 ± 0.7 cm^3 mol^{-1}). This difference between the R- and T-states implicates some different features of the CO rebinding mechanism between two quaternary states. Second, the activation volume for the T-state Hb was almost pressure independent, whereas that for the R-state Hb was reduced to nearly zero in going from 1 to 1000 bar.

To examine the pressure effects on the kinetic parameters, we also investigated the pressure dependence of the activation enthalpies and entropies for both R- and T-state Hbs. The temperature dependence of the association rate constants was studied at various pressures and some typical examples are shown in Figure 7. The plots are sufficiently linear to follow the Arrhenius equation (eq 4). The activation enthalpy and entropy were determined as described under Materials and Methods, and the pressure effects on them are listed in Table I. Upon elevating the pressure from 1 to 1000 bar, the activation enthalpy for the R-state Hb was increased from 18.4 ±0.1 to 20.7 ± 0.4 kJ mol^{-1} and the entropy was reduced from −14.7 ± 0.5 to −5.1 ± 1.5 J K^{-1} mol^{-1}. On the contrary, the activation enthalpy for the T-state Hb was decreased from 27.4 ± 1.2 to 21.4 ± 1.6 kJ mol^{-1} and the entropy was raised from −10.0 ± 4.0 to −23.4 ± 5.6 J K^{-1} mol^{-1} in going from 1 to 800 bar. The plots of $\Delta H^{\ddagger}$ and $-T\Delta S^{\ddagger}$ versus pressure at 293.15 K are illustrated in Figure 8.

Discussion

Pressure Effects on the Fraction of R- and T-State Hemoglobins. As illustrated in Figure 3, the fraction of the R-state Hb in the photodissociated Hb is increased by pressure, whereas that of the T-state Hb is reduced at high pressure. Such drastic proportional changes between the R- and T-state Hbs were also encountered for the partial photolysis experi-

Table I: Activation Enthalpy ($\Delta H^{\ddagger}$) and Entropy ($\Delta S^{\ddagger}$ and $-T\Delta S^{\ddagger}$) as a Function of Pressure for R- and T-State Hemoglobins[a]

	R-state Hb			T-state Hb		
P (bar)	$\Delta H^{\ddagger}$ (kJ mol^{-1})	$\Delta S^{\ddagger}$ (J K^{-1} mol^{-1})	$-T\Delta S^{\ddagger}$ (kJ mol^{-1})[b]	$\Delta H^{\ddagger}$ (kJ mol^{-1})	$\Delta S^{\ddagger}$ (J K^{-1} mol^{-1})	$-T\Delta S^{\ddagger}$ (kJ mol^{-1})[b]
1	18.4 ± 0.1	−14.7 ± 0.5	4.3 ± 0.1	27.4 ± 1.2	−10.0 ± 4.0	2.9 ± 1.2
200	18.4 ± 0.3	−14.2 ± 0.9	4.2 ± 0.3	25.0 ± 1.0	−16.0 ± 3.4	4.7 ± 1.0
400	17.9 ± 0.4	−15.3 ± 1.3	4.5 ± 0.4	23.2 ± 1.2	−19.8 ± 4.1	5.8 ± 1.2
600	19.4 ± 0.3	−10.1 ± 0.9	3.0 ± 0.3	21.5 ± 1.5	−24.3 ± 5.1	7.1 ± 1.5
800	20.5 ± 0.4	−5.9 ± 1.2	1.7 ± 0.4	21.4 ± 1.6	−23.4 ± 5.6	6.8 ± 1.6
1000	20.7 ± 0.4	−5.1 ± 1.5	1.5 ± 0.4			

[a] Experimental conditions were 50 mM Tris–0.1 M Cl$^-$, pH 7. Rate constants were obtained at various pressures in the temperature range from ~5 to ~25 °C. The values presented in this table were determined as described in Figures 4 and 5 (see text). The errors are listed as the standard deviation from the mean. The values for the T-state Hb at 1000 bar were not obtained, because the amplitudes of the slow components were markedly decreased. [b] 293.15 K was used for the value of T.

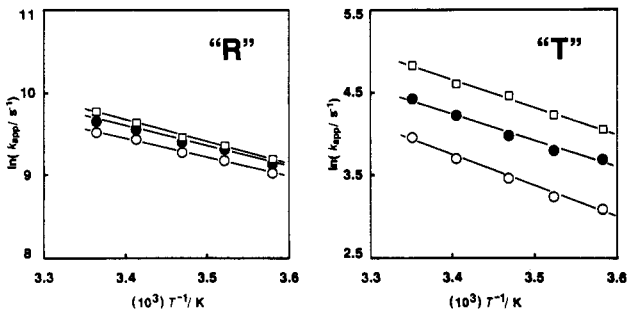

FIGURE 7: Plots of k_{app} versus $1/T$ for the bimolecular CO recombination reaction with the R- (left) and T- (right) state Hbs under various pressure: (○) 1 bar; (●) 400 bar; (□) 800 bar. k_{app} were evaluated by the Guggenheim plot method for the R-state Hb and by the semilog plot method for the T-state Hb. The temperature range was ~5–25 °C for all experiments.

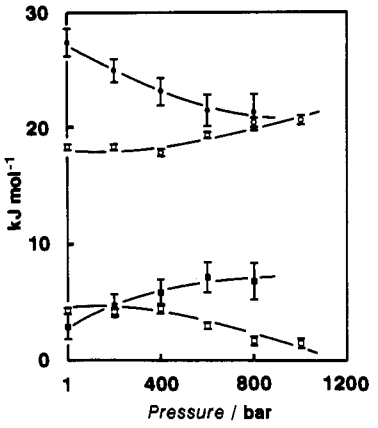

FIGURE 8: Pressure effects on the activation enthalpy ($\Delta H^{\ddagger}$) and the activation entropy term ($-T\Delta S^{\ddagger}$) for the bimolecular CO association reaction. The points and error bars were taken from Table I. For the enthalpy: (○) R; (●) T. For the entropy: (□) R; (■) T.

ments (Antonini et al., 1972; Sawicki & Gibson, 1976). In the partial photolysis experiment, reduction of the laser power resulted in a decrease in the intrinsic photodissociation rate, leading to an increase in the fraction of the partially photodissociated R-state Hb and a decrease in the fraction of the fully photodissociated T-state Hb. As shown in Figure 9, the dependencies of the fractional changes between the R- and T-state Hbs on the photodissociation in the partial photolysis experiment (Antonini et al., 1972; Schmelzer et al., 1972) were almost all the same as in the high-pressure photolysis experiment. It therefore follows that pressurization tends to increase the fraction of partially photodissociated Hb as found upon reduction of the laser power. It is well-known that the increase of the partially photodissociated Hb is induced by reduction of the intrinsic photodissociation rate in the partial photolysis experiment. However, in the high-pressure experiment, pressure increases the fraction of the geminate rebinding

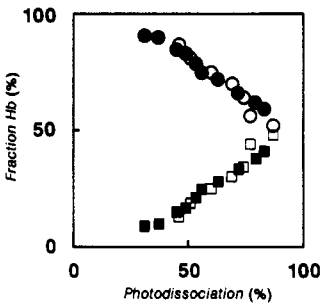

FIGURE 9: Fraction of the R- and T-state Hb (as a percentage of photodissociated Hb) plotted versus photodissociation of HbCO. The fraction of the R- and T-state Hb and the fraction of the photodissociated HbCO were determined in a manner similar to that in Figure 3. For the high-pressure experiments: (○) R; (□) T. For the partial photolysis experiments: (●) R; (■) T. Experimental conditions are listed in Figure 1.

concurrent with a decrease in the apparent quantum yield for the millisecond process as illustrated in Figure 2.

Since the geminate rebinding occurs before the transition from the R to T quaternary structure (Sawicki & Gibson, 1976; Murray et al., 1988a,b; Su et al., 1989), the increase of the geminate rebinding accompanied with the decrease of the millisecond rebinding induces the increase in the partially liganded R-state Hb and the decrease in the fully deoxygenated T-state Hb. Another alternate interpretation of the fractional changes between the R- and T-state Hb is that the transition rate from the R- to T-state is slowed down by pressurization. However, since the pressure and partial photolysis experiments gave nearly the same fractional changes, it is unlikely that the pressure drastically affects the R to T quaternary transition rates.

Dynamics of CO Binding to Hemoglobin—Activation Volumes. The following simple three-species scheme (Alpert et al., 1979; Campbell et al., 1984, 1985; Catterall et al., 1982; Duddell et al. 1979, 1980) was proposed to describe CO binding to Hb:

$$\mathrm{HbCO} \overset{1}{\rightleftharpoons} \mathrm{Hb{\cdot}CO} \overset{2}{\rightleftharpoons} \mathrm{Hb} + \mathrm{CO}$$

HbCO represents the CO-bound state; Hb·CO, the geminate state where CO is still in the heme pocket; and Hb + CO, a state where CO is in the solvent phase. According to this model, there are two elementary steps in the bimolecular CO association reaction, that is, the iron–ligand bond formation step (1) and the migration of the ligand molecule to the heme pocket (2).

It has been reported that the bond formation reaction of neutral molecules has a negative activation volume of the order of ca. −10 cm^3 mol^{-1} (le Noble, 1965) and the diffusion-controlled reaction such as CO binding to protoheme in aqueous ethylene glycol and in glycerol experiences positive activation volumes, +2 and +14 cm^3 mol^{-1}, respectively (Caldin &

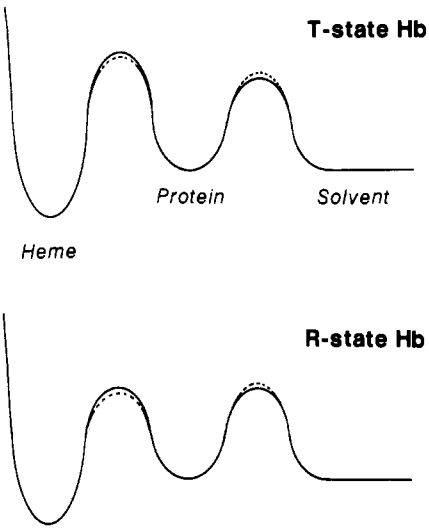

FIGURE 10: Relative free energies are plotted versus the reaction coordinate, taken as the distance between the heme iron and the ligand. The solid curves are at atmospheric pressure, while the dashed curves are at high pressure.

Hasinoff, 1975). The relationship between the activation volume and the rate-limiting steps was suggested by the studies of the pressure effects on the ligand binding to myoglobin (Hasinoff, 1974; Adachi & Morishima, 1989; Projahn et al., 1990). The negative activation volume was found (ca. -9 cm^3 mol^{-1}) for the CO binding reaction to sperm whale myoglobin in which the rate-limiting step is the bond formation process (Gibson et al., 1986), and the positive value ($\sim$5–8 cm^3 mol^{-1}) was obtained for O_2 binding to sperm whale myoglobin in which the rate-limiting step is the ligand migration process (Gibson et al., 1986). The activation volumes for the R- and T-state Hbs at atmospheric pressure are -9.0 ± 0.7 and -31.7 ± 2.4 cm^3 mol^{-1}, respectively. Such negative activation volumes suggest that the iron–ligand bond formation process affects the overall bimolecular association rate for the R- and T-state Hbs at ordinary pressure, which was previously suggested by Murray et al. (1988a,b).

However, of much interest is the different pressure dependence of the activation volumes for the R- and T-state Hbs. Figure 6 shows that the activation volume for the T-state Hb is almost constant at various pressures, whereas for the R-state Hb the activation volume at high pressure (>1000 bar) is rather close to zero. Since the ligand migration step prefers a negative activation volume, it is likely that the ligand migration step contributes to the rate-limiting process for the R-state Hb at high pressure, implying that the pressure reduces the ligand migration rate and accelerates the bond formation rate. Although we cannot rule out the possibility that the pressure-induced activation volume change is caused by a simple conformational change which does not affect the rate-limiting step, the pressure-induced increase of geminate rebinding also supports the reduction of the ligand migration rate by pressurization. For the T-state Hb, however, the pressure does not appear to affect the rate-limiting step so much as that for the R-state Hb. To discuss such quite different behaviors of pressure dependence between two quaternary structures, we utilize the free-energy diagram of the ligand binding process.

By referring to the results of CO binding kinetics for Fe–Co hybrid Hb (Murray et al., 1988a,b), we are able to show the schematic free energy diagrams for binding of CO to Hb in Figure 10. For the T-state Hb, the bond formation reaction at the heme iron is the rate-limiting step, whereas bond formation and ligand migration processes appear to contribute comparatively to rate determining for the R-state Hb. When the bond formation rate is accelerated and the ligand migration rate is slowed down by pressure for both quaternary structures as mentioned above, are able to depict the free energy diagrams at high pressure with the dashed curves in Figures 10. The free energy barrier between HbCO and Hb·CO is lowered and the barrier between Hb·CO and Hb + CO is raised by pressurization, which may explain the pressure-induced switching of the rate-limiting step from bond formation to migration for the R-state Hb. For the T-state Hb, however, no change of the rate-limiting step is caused by pressure, because the difference in the free energy barrier between the two processes is too large to be affected. This explanation appears to be further supported by our finding that the pressure induces an increase in the geminate yield. That is, the lowered free energy barrier for the bond formation at high pressure led to an increase in the geminate yield. The free energy diagrams in Figure 10 help us to interpret the different features of the high-pressure kinetics between two quaternary structures, although the effects of pressure on the rate of the elementary steps have not yet been clearified.

Pressure Effects on the Kinetic Parameters—Activation Enthalpy and Entropy. It has previously been reported that positive and negative activation volumes often correspond to positive and negative activation entropies, respectively (van Eldik et al., 1989). This correlation has also been obtained for the ligand binding reaction of myoglobin by Hasinoff (1974), who showed that the CO binding reaction with myoglobin experiences a negative activation volume (ca. -9 cm^3 mol^{-1}) and a large negative activation entropy (-81 J K^{-1} mol^{-1}), while the O_2 recombination reaction exhibits a positive activation volume ($\sim$5–8 cm^3 mol^{-1}) and a smaller negative activation entropy (-12 J K^{-1} mol^{-1}). Our present finding that the activation entropy for the R-state Hb is changed from ca. -15 at 1 bar to ca. -5 J K^{-1} mol^{-1} at 1000 bar appears to correspond to the pressure-induced changes of activation volume from ca. -9 to $\sim$0 cm^3 mol^{-1}. Since the reduction of the activation volume is considered to be caused by the competitive contribution of both bond formation and ligand migration processes to the rate-limiting step, such changes in the activation entropy could be due to the alteration of the rate-limiting step.

In contrast to that of the R-state Hb, a quite different pressure dependence of the activation enthalpy and entropy was observed for the T-state Hb. Table I and Figure 8 show that for the T-state Hb the pressure (800 bar) caused an $\sim$6 kJ mol^{-1} increase in the activation enthalpy and an $\sim$13 J K^{-1} mol^{-1} decrease in the activation entropy. Since the pressure effects are opposite between the two quaternary state Hbs, the pressure effects on the activation enthalpy and entropy for the T-state Hb may result from the structural changes around the heme cavity rather than the alteration of the rate-limiting step. Our previous study suggested that the structural changes of the T-state Hb are affected by pressurization more effectively than those of the R-state Hb (Morishima & Hara, 1983). However, it is unlikely that the pressure induces drastic structural changes for the T-state Hb. In fact, our high-pressure NMR study (Morishima & Hara, 1983) also showed that the pressure only affects the local tertiary structure, but not the quaternary structure. Such a small enthalpy change was encountered for the single amino acid substituted myoglobin (Braunstein et al., 1988). Comparison of the CO rebinding rate between wild-type and a synthetic mutant myoglobin where the distal histidine (His-E7) was replaced by

glycine suggested that the replacement effect of His-E7 amounts to 4 kJ mol^{-1} of the low enthalpy barrier. Therefore, the pressure-induced free energy changes in the R- and T-state Hbs could result from pressure-induced subtle structural changes but not from the global alteration of the whole protein structure.

In summary, the most characteristic feature of the present high-pressure laser photolysis experiments of HbCO A is the decrease of the millisecond apparent quantum yield. This pressure sensitivity is caused by an increase in the fraction of the nanosecond recombination reaction, and it is suggested that pressure does not affect the intrinsic photodissociation rate. The pressure and partial photolysis experiments gave nearly the same fractional changes, showing a little pressure effect on the R to T quaternary transition rates. The different activation volumes and their pressure dependence between the two quaternary structures, the R- and T-states, imply that the dynamic state for the ligand binding is different between the two quaternary states. For the R-state Hb, CO migration through the protein contributes more to the rate-limiting step at high pressure. The pressure-dependent activation entropy also supports our conclusion that high pressure changes the rate-limiting step for the R-state Hb.

Acknowledgments

We thank Prof. K. Hamanoue, Dr. T. Nakayama, and Dr. K. Ushida (Kyoto Institute of Technology) for the nanosecond laser photolysis measurement and Dr. K. Hara (Kyoto University) for the high-pressure experiment.

Registry No. Hb A, 9034-51-9; CO, 630-08-0.

References

Adachi, S., & Morishima, I. (1989) *J. Biol. Chem. 264*, 18896–18901.

Alden, R. G., Satterlee, J. D., Mintorovitch, J., Constantindis, I., Ondrias, M. R., & Swanson, B. I. (1989) *J. Biol. Chem. 264*, 1933–1940.

Alpert, B., El Mohsni, S., Lindqvist, L., & Tfibel, F. (1979) *Chem. Phys. Lett. 64*, 11–16.

Antonini, E., & Brunori, M. (1971) *Hemoglobin and Myoglobin in Their Reaction with Ligands*, North-Holland, Amsterdam.

Antonini, E., Anderson, N. M., & Brunori, M. (1972) *J. Biol. Chem. 247*, 319–321.

Austin, R. H.; Beeson, K. W., & Frauenfelder, H. (1975) *Biochemistry 14*, 5355–5373.

Baldwin, J. M.; & Chothea, C. (1979) *J. Mol. Biol. 129*, 175–201.

Braunstein, D., Ansari, A., Berendzen, J., Cowen, B. R., Egeberg, K. D., Frauenfelder, H., Hong, M. K., Ormos, P., Sauke, T. B., Scholl, R., Schulte, A., Sligar, S. G., Springer, B. A., Steinbach, P. J., & Young, R. D. (1988) *Proc. Natl. Acad. Sci. U.S.A. 85*, 8497–8501.

Caldin, E. F., & Hasinoff, B. B. (1975) *J. Chem. Soc., Faraday Trans. 1 71*, 515–527.

Campbell, B. F., Magde, D., & Sharma, V. S. (1984) *J. Mol. Biol. 179*, 143–150.

Campbell, B. F., Magde, D., & Sharma, V. S. (1985) *J. Biol. Chem. 260*, 2752–2756.

Catterall, R., Duddell, D. A., Morris, R. J., & Richards, J. T. (1982) *Biochim. Biophys. Acta 705*, 257–263.

Duddell, D. A., Morris, R. J., & Richards, J. T. (1979) *J. Chem. Soc., Chem. Commun.*, 75–76.

Duddell, D. A., Morris, R. J., & Richards, J. T. (1980) *Biochim. Biophys. Acta 621*, 1–8.

Frauenfelder, H., Alberding, N. A., Ansari, A., Braunstein, D., Cowen, B. R., Hong, M. K., Iben, I. E. T., Johnson, J. B., Luck, S., Maredn, M. C., Mourant, J. R., Ormos, P., Reinisch, L., Scholl, R., Schulte, A., Shyamusnder, E., Sorensen, L. B., Steinbach, P. J., Xie, A., Young, R. D., & Yue, K. T. (1990) *J. Phys. Chem. 94*, 1024–1937.

Friedman, J. M., & Lyons, K. B. (1980) *Nature (London) 284*, 570–572.

Gibson, Q. H. (1959a) *Biochem. J. 71*, 293–303.

Gibson, Q. H. (1959b) *Prog. Biophys. Biophys. Chem. 9*, 1–53.

Gibson, Q. H., Olson, J. S., McKinnie, R. E., & Rohlfs, R. J. (1986) *J. Biol. Chem. 261*, 10228–10239.

Glasstone, S., Laidler, K. J., & Eyring, H. (1941) *The Theory of Rate Processes*, McGraw-Hill, New York.

Hara, K., & Morishima, I. (1988) *Rev. Sci. Instrum. 59*, 2397–2398.

Hasinoff, B. B. (1974) *Biochemistry 13*, 3111–3117.

Hofrichter, J., Sommer, J. H., Henry, E. R., & Eaton, W. A. (1983) *Proc. Natl. Acad. Sci. U.S.A. 80*, 2235–2239.

Ishimori, K., & Morishima, I. (1988) *Biochemistry 27*, 4060–4066.

le Noble, W. J. (1965) *Prog. Phys. Org. Chem. 5*, 207–330.

Messana, C., Cerdania, M., Shenkin, P., Nable, R. W., Fermi, G., Perutz, R. N., & Perutz, M. F. (1978) *Biochemistry 17*, 3652–3662.

Morishima, I., & Hara, M. (1982) *J. Am. Chem. Soc. 104*, 6833–6834.

Morishima, I., & Hara, M. (1983) *J. Biol. Chem. 258*, 14428–14432.

Morishima, I., Ogawa, S., & Yamada, H. (1979) *J. Am. Chem. Soc. 101*, 7074–7076.

Morishima, I., Ogawa, S., & Yamada, H. (1980) *Biochemistry 19*, 1569–1575.

Murray, L. P., Hofrichter, J., Henry, E. R., Ikeda-Saito, M., Kitagishi, K., Yonetani, T., & Eaton, W. A. (1988a) *Proc. Natl. Acad. Sci. U.S.A. 85*, 2151–2155.

Murray, L. P., Hofrichter, J., Henry, E. R., & Eaton, W. A. (1988b) *Biophys. Chem. 29*, 63–76.

Neuman, R. C., Jr., Kauzmann, W., & Zipp, A. (1973) *J. Phys. Chem. 77*, 2687–2691.

Ogunmola, G. B., Zipp, A., Chen, F., & Kauzmann, W. (1977) *Proc. Natl. Acad. Sci. U.S.A. 74*, 1–4.

Perutz, M. F. (1980) *Proc. R. Soc. London, Ser. B 208*, 135–162.

Projahn, H.-D., Dreher, C., & van Eldik, R. (1990) *J. Am. Chem. Soc. 112*, 17–22.

Sawicki, C. A., & Gibson, Q. H. (1976) *J. Biol. Chem. 251*, 1533–1542.

Schmelzer, U., Steiner, R., Mayer, A., Nedetzka, T., & Fasold, H. (1972) *Eur. J. Biochem. 25*, 491–497.

Su, C., Park, Y. D., Liu, G.-Y., & Spiro, T. G. (1989) *J. Am. Chem. Soc. 111*, 3457–3459.

Szabo, A. (1978) *Proc. Natl. Acad. Sci. U.S.A. 75*, 2108–2111.

van Eldik, R., Asano, T., & le Noble, W. J. (1989) *Chem. Rev. 89*, 549–688.

Weber, G., & Drickamer, H. G. A. (1983) *Rev. Biophys. 16*, 89–95.